

Outlier detection by ensembling uncertainty with negative objectness

Anja Delić^{*1} Matej Grcić^{*1} Siniša Šegvić^{*1}

Abstract

Outlier detection is an essential capability in safety-critical applications of supervised visual recognition. Most of the existing methods deliver best results by encouraging standard closed-set models to produce low-confidence predictions in negative training data. However, that approach conflates prediction uncertainty with recognition of the negative class. We therefore reconsider direct prediction of $K+1$ logits that correspond to K groundtruth classes and one outlier class. This setup allows us to formulate a novel anomaly score as an ensemble of in-distribution uncertainty and the posterior of the outlier class which we term negative objectness. Now outliers can be independently detected due to i) high prediction uncertainty or ii) similarity with negative data. We embed our method into a dense prediction architecture with mask-level recognition over $K+2$ classes. The training procedure encourages the novel $K+2$ -th class to learn negative objectness at pasted negative instances. Our models outperform the current state-of-the-art on standard benchmarks for image-wide and pixel-level outlier detection with and without training on real negative data.

1. Introduction

Outliers correspond to test examples that strongly deviate from the training distribution (Hawkins, 1980). They are closely related to anomalies and novelties that also correspond to low-probability regions of the input space and call for the same detection methods (Ruff et al., 2021). Furthermore, they differ from typical effects of the domain shift (Sakaridis et al., 2021) due to substantial textural or semantic novelty. We are especially interested in detecting semantic outliers in the strongly supervised context (Shalev

et al., 2018; Bevandić et al., 2022). Recent surge of interest in such methods suggests that they represent an important missing piece in the deep learning puzzle (Zhang et al., 2023b; Blum et al., 2021; Chan et al., 2021a).

Many practical applications of visual recognition train or fine-tune on pre-defined taxonomies (Lin et al., 2014; Zhou et al., 2019) in the closed-set setup (Geng et al., 2020). Thus, their real-world performance may become unpredictable in presence of anomalous objects (Zendel et al., 2018). Outlier detection enables graceful performance degradation by allowing the classifier to decline the decision in unknown visual concepts (Zhang et al., 2020; Liang et al., 2022). Typically, the outlier detector delivers a scalar anomaly score that allows to rank outliers and to evaluate them with respect to some threshold (Ruff et al., 2021).

Negative training data represents an important component of recent anomaly detectors both in the image-wide (Hendrycks et al., 2018; Dhamija et al., 2018) and the pixel-level context (Bevandić et al., 2022; Biase et al., 2021; Chan et al., 2021b; Grcić et al., 2022; Tian et al., 2022). Although it cannot represent the entire variety of the visual world, the negative data can still help by signaling that not all data should be confidently recognized. If the variety of the negative data exceeds the variety of the inliers, then there is a reasonable hope that the test outliers will be detected. Unfortunately, this entails unwanted bias towards outliers that appear similar to the negative data. This concern can be addressed either by relying on synthetic negatives (Lee et al., 2018; Neal et al., 2018), or through separate ranking of approaches that do not train on real negative data (Zhang et al., 2023b; Blum et al., 2021; Chan et al., 2021a).

This paper focuses on outliers that may be missed by previous discriminative methods (Hendrycks et al., 2018; Dhamija et al., 2018) due to being dissimilar to negative data. We build upon a key observation that these outliers tend to yield highly uncertain predictions in the $K+1$ multi-class setup. We will assume that the first K logits correspond to inlier classes while the remaining $K+1$ -th logit represents the outliers. Interestingly, this non-standard setup did not underperform with respect to standard K -way performance in any of our experiments. Consequently, we propose a novel anomaly score that ensembles *negative objectness* $s_{NO} = P(K + 1 | \mathbf{x})$ with uncertainty over K inlier classes

¹University of Zagreb, Faculty of Electrical Engineering and Computing, Unska 3, 10000 Zagreb, Croatia. Correspondence to: Anja Delić <anja.delic@fer.hr>, Matej Grcić <matej.grcic@fer.hr>, Siniša Šegvić <siniša.segvic@fer.hr>.

$s_{\text{Unc}} = -\max_{k \leq K} P(k|\mathbf{x})$ (Hendrycks & Gimpel, 2017).

Our approach is a remarkably good fit in the pixel-level context as extension of some direct set-prediction approach (Cheng et al., 2022; Yu et al., 2022; Li et al., 2023). In particular, we propose to learn negative objectness as the mask-level posterior of the $K+2$ -th class, and to formulate pixel-level anomaly scores by ensembling the corresponding mask-level cues (Grcić et al., 2023). A closer look suggests that our score performs well due to different inductive bias of its two components as indicated by a remarkably weak correlation. Our concept performs competitively in the image-wide context as well, even though the absence of the no-object class leads to somewhat stronger correlation of the two components. Our models outperform the current state-of-the-art on several standard benchmarks in both learning setups, i.e. with and without real negative data.

2. Related work

Our related work comprises image-wide OOD detection (Sec. 2.1) and per-pixel OOD detection based on mask-level recognition (Sec. 2.3).

2.1. Image-wide outlier detection

We can distinguish three main categories among image-wide outlier detection methods: post-hoc inference methods, training methods without negative data, and training methods with negative data. The post-hoc inference methods build inference phase OOD scores on top of closed-set classifiers which are trained using the standard cross-entropy loss. The baseline methods model the outlier score as maximum softmax probability (Hendrycks & Gimpel, 2016) or maximum logit (Hendrycks et al., 2019a) over in-distribution classes. TempScale (Guo et al., 2017) calibrates softmax probabilities with temperature scaling while ODIN (Liang et al., 2017) further introduces input preprocessing. Recent post-hoc methods simplify layer activations (Djurisic et al., 2022) or base their score on template distances (Zhang et al., 2022).

In contrast, training methods involve training-time regularization either considering only inlier data or utilizing real negative data. OE (Hendrycks et al., 2018) is the first method following that setup that introduced outlier exposure by requiring low entropy for inlier classes given an outlier example. MCD (Yu & Aizawa, 2019) considers two classification heads with different decision boundaries and the training procedure promotes discrepancy between each head’s prediction on OOD samples. UDG (Yang et al., 2021) uses a clustering method to group auxiliary data to ID taxonomy to enrich semantic knowledge of ID classes. MixOE (Zhang et al., 2023a) mixes ID data and training outliers to expand the coverage of different OOD examples, and trains

the model such that the prediction confidence decays as the input transitions from ID to OOD. Some representatives of training methods that do not use negative data are RotPred (Hendrycks et al., 2019b), LogitNorm (Wei et al., 2022) and NPOS (Tao et al., 2023).

2.2. Pixel-level anomaly detection

Some image-wide anomaly detection methods can be directly applied in to pixel-level anomaly detection such as MSP (Hendrycks & Gimpel, 2016) and max-logit (Hendrycks et al., 2019a) and are considered as baseline methods. The early approaches for anomaly detection are based on estimating the prediction uncertainty using maximum softmax probability (Hendrycks & Gimpel, 2017), ensembling (Lakshminarayanan et al., 2017) or Bayesian uncertainty (Mukhoti & Gal, 2018). Subsequent work suggests using energy scores (Liu et al., 2020) or standardizing max-logit (Jung et al., 2021). Recent high-performing approaches train on mixed images with pasted negative crops or instances (Biase et al., 2021; Chan et al., 2021b; Grcić et al., 2022; Hendrycks et al., 2018; Tian et al., 2022; Bevandić et al., 2022). This can be interpreted as a regularisation method where the model is exposed to a broad negative dataset. Real negative data can be replaced with synthetic negative patches obtained by sampling a jointly trained generative model (Lee et al., 2018; Neal et al., 2018; Zhao et al., 2021). Anomaly detection performance can be further improved by supplying more capacity (Vaze et al., 2021). An interesting recent approach leverages generic pre-trained representations (Vojir et al., 2023).

A very interesting application of generative models is their use for out-of-distribution detection. Generative methods detect outliers according to the estimated density of the generative distribution of the inlier training data. The data likelihood has been estimated by a normalizing flow (Dinh et al., 2017; Blum et al., 2021) or by leveraging an energy-based model (Grcić et al., 2022). However, estimating the data likelihood with a generative model can be suboptimal because the generative model may assign higher likelihood to outliers than inliers (Nalisnick et al., 2019; Kirichenko et al., 2020). Nevertheless, useful performance can be obtained by modelling the density of semantic features (Zhang et al., 2020).

2.3. Outlier detection methods that build upon Mask2Former

Recent panoptic architectures (Cheng et al., 2022; Yu et al., 2022; Li et al., 2023) decompose scene understanding into class-agnostic segmentation and region-wide recognition. They frame the detection of semantic regions as direct set-prediction where each mask is classified into K inlier classes and one no-object class. Consequently, this architecture has

a built in degree of openness which favours outlier detection.

Recent work shows great applicability of the Mask2Former architecture for segmentation in presence of outliers (Nayal et al., 2023; Rai et al., 2023; Ackermann et al., 2023; Grcić et al., 2023). The RbA (Nayal et al., 2023) approach proposes an outlier score as the probability of not belonging to any of the known classes. The model is based on mask-level recognition but the scoring function is defined in a per-pixel manner. The mask decoder is fine-tuned by reducing energy in the negative pixels.

Another interesting method is the Mask2Anomaly (Rai et al., 2023) model that introduces adaptation of the initial Mask2Former model in architecture, training and inference. They introduce a global mask-attention which allows the model to focus on both foreground and background and finetune the model in a contrastive manner to maximize the separation of inliers and negatives in terms of max-softmax score. We note that they introduce a very strong, dataset-specific assumption that anomalies in traffic scenes appear only on the road, which is why they refine the predictions at inference by masking all stuff classes except the road.

Maskomaly (Ackermann et al., 2023) leverages the fact that masks specialize for detecting specific object categories which means that we can also select masks that capture anomalous objects by thresholding the per-class mIoU on the anomaly detection validation sets. Maskomaly is interesting because it does not require training on negative data but its main disadvantage is that it requires a test subset for selecting the anomaly mask.

Contrary to previously mentioned approaches (Nayal et al., 2023; Rai et al., 2023; Ackermann et al., 2023), EAM (Grcić et al., 2023) proposes to detect anomalies by ensembling mask-level scores. EAM can be enhanced by fine-tuning the model to discourage the masks to capture negative instances.

3. Learning negative objectness

Our method assumes that a broad negative dataset is available in addition to the inlier dataset with K labeled classes. We extend a closed-set classifier with an additional $K+1$ -th class for the negative examples and formulate negative objectness as the posterior of the $K+1$ -th class. We train the extended classifier by minimizing cross-entropy over $K+1$ classes.

We propose a novel anomaly score, given pre-logits \mathbf{z} , which can be interpreted as an ensemble of in-distribution uncertainty and negative objectness:

$$s_{\text{UNO}}(\mathbf{z}) = s_{\text{Unc}}(\mathbf{z}) + s_{\text{NO}}(\mathbf{z}). \quad (1)$$

The in-distribution uncertainty score s_{Unc} corresponds to negative max-softmax of K inlier classes or, equivalently,

the negative probability of the winning inlier class \hat{k} :

$$\begin{aligned} s_{\text{Unc}}(\mathbf{z}) &= -\max_{k=1\dots K} P(Y = k|\mathbf{z}) \\ &= -\max_{k=1\dots K} \frac{\exp(\mathbf{w}_k \mathbf{z})}{\sum_{j=1}^{K+1} \exp(\mathbf{w}_j \mathbf{z})} \\ &= -\frac{\exp(\mathbf{w}_{\hat{k}} \mathbf{z})}{\sum_{j=1}^{K+1} \exp(\mathbf{w}_j \mathbf{z})}. \end{aligned} \quad (2)$$

On the other hand, s_{NO} corresponds to the posterior of the $K+1$ -th class which models the negative objectness:

$$\begin{aligned} s_{\text{NO}}(\mathbf{z}) &= P(Y = K + 1|\mathbf{z}) \\ &= \frac{\exp(\mathbf{w}_{K+1} \mathbf{z})}{\sum_{j=1}^{K+1} \exp(\mathbf{w}_j \mathbf{z})}. \end{aligned} \quad (3)$$

We denote our method as ensemble of Uncertainty and Negative Objectness (UNO).

Our ensemble recognizes outliers when the corresponding pre-logit \mathbf{z} either has a small L2 norm or a large projection onto the $K+1$ -th vector of the weight vector \mathbf{w}_{K+1} within the pre-softmax layer:

$$s_{\text{UNO}}(\mathbf{z}) \propto -\exp(\mathbf{w}_{\hat{k}} \mathbf{z}) + \exp(\mathbf{w}_{K+1} \mathbf{z}). \quad (4)$$

The s_{Unc} score captures anomalies with a low embedding norm because it assumes that anomalies give rise to examples with high recognition uncertainty. On the other hand, the s_{NO} score captures anomalies that are confidently classified into the $K+1$ -th class due to clear association with the negative training data. Figure 1 displays a histogram of the mask-level pre-logit L2-norms across detected anomalous

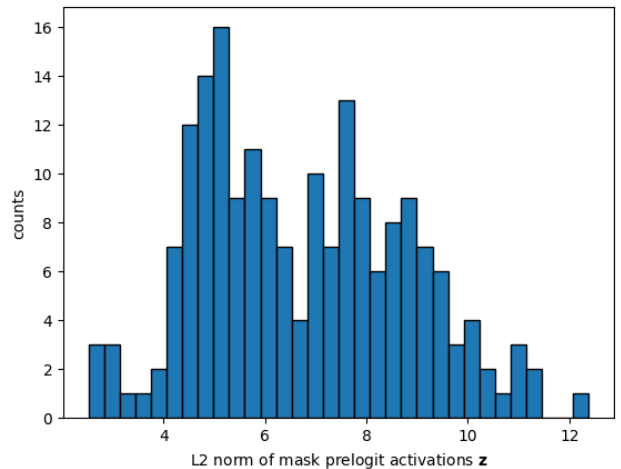


Figure 1. Histogram of L2-norms of the mask pre-logit activations at pixels with the highest s_{Unc} score on Fishyscapes validation sets and RoadAnomaly.

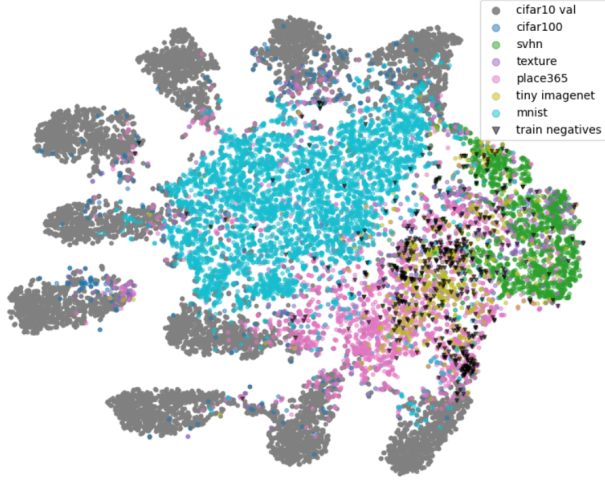


Figure 2. A two-dimensional t-SNE projection of pre-logit embeddings from a ResNet-18 with $K+1$ classes trained on CIFAR-10 and evaluated on the OpenOOD CIFAR10. We observe that some outliers are quite far from the training negatives.

pixels on the validation images from Fishyscapes and Road-Anomaly. We clearly observe two modes in the histogram, which reflects the above discussion.

Figure 2 shows a two-dimensional projection of pre-logit embeddings \mathbf{z} from a ResNet-18 with $K+1$ classes trained on one Open-OOD CIFAR-10. We observe that the in-distribution data is clustered as expected (grey circles) and that the train negatives are placed near related outliers. Please note that train negatives are a subset of the Tiny ImageNet dataset. We clearly observe that some outliers are closer to the train negatives than others. We expect that outliers that are relatively close to the train negative data will be detected by the score s_{NO} while the more dissimilar outliers will be detected by the score s_{Unc} .

Our proposed training procedure and anomaly score can be applied for both image-wide and pixel-level outlier detection. Implementation in the image-wide setup is straight forward. It is only required to change the last fully connected layer of a deep convolutional model by adding one additional class. In the pixel-level setup we implement our method on top of the Mask2Former model (Cheng et al., 2022) and use the UNO ensemble as a mask-wide anomaly score.

4. Scene parsing with mask-wide recognition

The Mask2Former (Cheng et al., 2022) architecture consists of three main parts: backbone, pixel decoder, and mask decoder. The backbone extracts features at multiple scales from a given image $\mathbf{x} \in \mathbb{R}^{3 \times H \times W}$. The pixel decoder pro-

duces high-resolution per-pixel features $\mathbf{E} \in \mathbb{R}^{E \times H \times W}$ that are fed into the mask decoder. The mask decoder formulates semantic segmentation as a direct-set prediction problem by providing two outputs: N mask embeddings \mathbf{q} , and N mask-wide categorical distributions over $K+1$ classes:

$$P(Y = k | \mathbf{z}_i) = \text{softmax}(\mathbf{W} \cdot \mathbf{z}_i). \quad (5)$$

The $K+1$ classes include K inlier classes and one no-object class. Please note that \mathbf{z}_i denotes the vector of mask-wide pre-logit activations of the i -th mask. The mask decoder projects pre-logits \mathbf{z}_i into logits by applying the learned matrix \mathbf{W} . We obtain binary masks \mathbf{m} by scoring per-pixel features \mathbf{E} with the mask embeddings \mathbf{q} :

$$\mathbf{m} = \sigma(\text{conv}_{1 \times 1}(\mathbf{E}, \mathbf{q})). \quad (6)$$

The sigmoid activation interprets each element of the obtained tensor as a probabilistic assignment of the particular pixel into the corresponding mask. Semantic segmentation can be carried out by classifying each pixel according to a weighted ensemble of per-mask classifiers $P(y | \mathbf{z})$, where the weights correspond to dense mask assignments \mathbf{m} :

$$\hat{y}[r, c] = \underset{k=1, \dots, K}{\text{argmax}} \sum_i^N \mathbf{m}_i[r, c] P(Y = k | \mathbf{z}_i). \quad (7)$$

The mask-level posterior (5) already includes $K+1$ classes that correspond to K inlier classes and one no-object class. We implement our method by introducing an additional class to learn the negative objectness, which brings us to $K+2$ classes in total. To be consistent with the image-wide setup, in addition to the K inlier classes, we place the outlier class at index $K+1$ and the no-object class at index $K+2$. We expose the segmentation model to negative data by training on mixed-content images. We obtain mixed-content images by pasting instances from the negative dataset atop inlier scenes (Biase et al., 2021; Chan et al., 2021b; Bevandić et al., 2022). Closed-set recognition can still be carried out by considering only the K inlier logits (7).

We detect anomalies on the mask-level by applying UNO to the mask-wide pre-logits \mathbf{z}_i of the i -th mask. Note that in this case of mask-wide anomaly detection the softmax in equations 2 and 3 considers all $K+2$ classes. We define the per-pixel anomaly score as a sum of mask-level anomaly scores weighted with with dense probabilistic mask assignments:

$$\mathbf{s}_{\text{UNO}}^{\text{M2F}}[r, c] = \sum_{i=1}^N \mathbf{m}_i[r, c] \cdot (s_{\text{Unc}}(\mathbf{z}_i) + s_{\text{NO}}(\mathbf{z}_i)). \quad (8)$$

5. Synthetic negatives

We consider to train our models on dynamically generated synthetic negative data. We assume a discriminative classifier parameterised by Θ and a generative normalizing flow

parameterised by Φ . We jointly train the normalizing flow with the classifier in order to generate samples at the border of the inlier manifold. We train the normalizing flow according to the following (Grcić et al., 2021a) loss:

$$L_{\text{flow}}(\Phi) = L_{\text{mle}}(\Phi) + \beta \cdot L_{\text{jsd}}(\Phi, \Theta). \quad (9)$$

The first term is the negative log-likelihood of inlier data D_{in} :

$$L_{\text{mle}}(\Phi) = -\mathbf{E}_{\mathbf{x} \in D_{\text{in}}} [\ln p_{\Phi}(\mathbf{x})]. \quad (10)$$

The second term corresponds to the Jensen-Shannon divergence between the posterior $P(Y|\mathbf{x})$ and uniform distribution while β denotes a loss modulation hyperparameter. The first term attracts the generative distribution towards inliers while the second term repels it from the inlier manifold. A normalizing flow trained by (9) generates data at the boundary of the training distribution. It is important to note that gradients of the loss $L_{\text{jsd}}(\Psi, \Theta)$ impact not only the flow but also the classifier. These gradients force the classifier to give uniform inlier posteriors in negative samples.

We incorporate this training paradigm to the training procedure proposed in the sections 3 and 4. Now we train the classifier to predict uncertain inlier posteriors in negative examples while simultaneously classifying them into the $K+1$ -th class. At the same time, the jointly trained normalizing flow learns to generate examples at the border of the inlier distribution.

6. Experiments

We present our experimental setup with implementation details (Sec. 6.1), per-pixel OOD detection (Sec. 6.2), image-wide OOD detection (Sec. 6.3), and ablation studies (Sec. 6.4).

6.1. Experimental setup

Baselines. We compare UNO with three groups of previous outlier detection methods. Image-wide methods operate atop image classification models such as MSP (Hendrycks & Gimpel, 2017) and OE (Hendrycks et al., 2018). Pixel-wise methods operate atop a per-pixel classifier such as SML (Jung et al., 2021) and JSRNet (Vojir et al., 2021). Finally, mask-level methods operate atop panoptic architectures with direct set-prediction such as EAM (Grcić et al., 2023) and RbA (Nayal et al., 2023). The complete list of baselines for each category can be found in the Appendix.

Benchmarks & Datasets. We evaluate the performance of UNO on standard image-wide and pixel-level outlier detection benchmarks. In the image-wide setup, we consider the OpenOOD benchmark (Zhang et al., 2023b). OpenOOD consists of two inlier datasets: CIFAR-10 (Krizhevsky et al., 2009) and ImageNet200 (Deng et al., 2009). The negative

training samples are sourced from TinyImageNet and ImageNet800, respectively. The test outliers originate from a collection of datasets and can be grouped into two categories. The far-OOD group consists of outliers that are semantically far from the inliers (e.g. MNIST and SVHN numbers). The near-OOD group consists of outliers that are semantically similar to the inliers, such as animals from NINCO (Bitterwolf et al., 2023).

In the case of pixel-level setup, we consider Fishyscapes (Blum et al., 2021) and SMIYC (Chan et al., 2021a), the two prominent benchmarks for semantic anomaly segmentation in road driving scenes. Fishyscapes contains datasets with real (FS L&F) and synthetic (FS Static) outliers. SMIYC has two dominant tracks which group anomalies according to size. AnomalyTrack focuses on the detection of large anomalies on the traffic scenes while ObstacleTrack focuses on the detection of small obstacles on the road.

Evaluation metrics. We use standard evaluation metrics: average precision (AP), area under the receiver operating curve (AUROC), and false positive rate at 95% true positive rate (FPR₉₅). We validate in-distribution performance with accuracy and mIoU.

Implementation details. Our image-wide experiments build upon a ResNet-18 (He et al., 2016) backbone with $K+1$ -way predictions and random initialization. We use the same training setup as in (Zhang et al., 2023b). Our pixel-level experiment build upon a Mask2Former model (Cheng et al., 2022) with an ImageNet-initialized SWIN-L (Liu et al., 2021) backbone. We pre-train the Mask2Former model in the closed-set setup for 115K iterations on Cityscapes (Cordts et al., 2016) and Mapillary Vistas (Neuhof et al., 2017) with the Cityscapes taxonomy. We extend the mask-wide classifier to $K+2$ classes and fine-tune the model on mixed-content images for 2K iterations. When training on real negative data, we create mixed-content images by pasting three randomly selected ADE20K (Zhou et al., 2019) instances atop inlier scene. In the case of synthetic negatives, we follow the NFlowJS procedure (Grcić et al., 2021a) and paste synthetic negatives generated by the jointly trained DenseFlow (Grcić et al., 2021c). We use the standard Mask2Former hyperparameters (Cheng et al., 2022) except for the batch size, which we set to 18. The closed-set training of Mask2Former lasts 48 hours, while the fine-tuning stage takes only 30 minutes on three A6000 GPUs.

6.2. Anomaly-aware segmentation of road scenes

Tables 1 and 2 compare UNO with the related work on Fishyscapes and SMIYC. The two sections divide methods that train on real negative data (bottom) or not (top). We observe that mask-level recognition methods deliver significant improvement over the earlier work. When training with

real negatives, our method outperforms all previous work on Fishyscapes and SMIYC AnomalyTrack while performing within variance of the top method on SMIYC ObstacleTrack. When training with synthetic negatives, our method outperforms all previous work on SMIYC and Fishyscapes Static by a large margin while achieving second best AP on Fishyscapes L&F.

Table 1. Experimental evaluation on the Fishyscapes benchmark. The top section presents methods that do not train on real negative data. Methods that build on MaskFormer are marked with †.

Method	FS Lost&Found		FS Static		City mIoU
	AP	FPR ₉₅	AP	FPR ₉₅	
Maximum Entropy	15.0	85.1	0.8	77.9	9.7
Image Resynthesis	5.7	48.1	29.6	27.1	81.4
Max softmax	1.8	44.9	12.9	39.8	80.3
SML	31.7	21.9	52.1	20.5	-
Embedding Density	4.3	47.2	62.1	17.4	80.3
NFlowJS	39.4	9.0	52.1	15.4	77.4
SynDHybrid	51.8	11.5	54.7	15.5	79.9
cDNP	62.2	8.9	-	-	-
EAM [†]	9.4	41.5	76.0	10.1	83.5
UNO [†] (ours)	<u>56.4</u>	55.1	91.1	1.5	83.5
SynBoost	43.2	15.8	72.6	18.8	81.4
Prior Entropy	34.3	47.4	31.3	84.6	70.5
OOD Head	30.9	22.2	84.0	10.3	77.3
Void Classifier	10.3	22.1	45.0	19.4	70.4
Dirichlet prior	34.3	47.4	84.6	30.0	70.5
DenseHybrid	43.9	6.2	72.3	5.5	81.0
PEBAL	44.2	7.6	92.4	1.7	-
cDNP	69.8	7.5	-	-	-
Mask2Anomaly [†]	46.0	4.4	95.2	0.8	-
EAM [†]	63.5	39.2	93.6	1.2	83.5
UNO (ours) [†]	74.8	2.7	95.8	0.3	83.7

Table 3 compares our method with other mask-level methods on validation subsets of Fishyscapes and RoadAnomaly (Lis et al., 2019). Our method outperforms all related approaches on all datasets while only having 0.5 pp worse FPR₉₅ than RbA on RoadAnomaly.

6.3. Image-wide OOD detection

Table 4 shows the image-wide performance of UNO on the OpenOOD benchmark (Zhang et al., 2023b). We compare UNO with the relevant baseline methods that train on negative data. In the case of CIFAR-10, UNO consistently outperforms all baselines on both far and near OOD detection. In the case of Imagenet-200, UNO outperforms all baselines in near OOD detection. For the far OOD detection, UNO attains the best AUROC and the second-best FPR. In addition, UNO preserves the inlier classification performance.

Table 2. Experimental evaluation on the SMIYC benchmark. The top section presents methods that do not train on real negative data. Methods that build on MaskFormer are marked with †.

Method	AnomalyTrack		ObstacleTrack	
	AP	FPR ₉₅	AP	FPR ₉₅
Image Resynthesis	52.3	25.9	37.7	4.7
JSRNet	33.6	43.9	28.1	28.9
Max softmax	28.0	72.1	15.7	16.6
MC Dropout	28.9	69.5	4.9	50.3
ODIN	33.1	71.7	22.1	15.3
Embedding Density	37.5	70.8	0.8	46.4
cDNP	88.9	11.4	72.70	1.40
EAM [†]	76.3	93.9	66.9	17.9
RbA [†]	86.1	15.9	87.8	3.3
Maskomaly [†]	93.4	6.9	-	-
UNO (ours) [†]	96.1	2.3	89.0	0.6
SynBoost	56.4	61.9	71.3	3.2
DenseHybrid	78.0	9.8	78.7	2.1
PEBAL	49.1	40.8	5.0	12.7
Void Classifier	36.6	63.5	10.4	41.5
Maximum Entropy	85.5	15.0	85.1	0.8
RbA [†]	90.9	11.6	91.8	0.5
EAM [†]	93.8	4.1	92.9	0.5
Mask2Anomaly [†]	88.7	14.6	93.3	0.2
UNO (ours) [†]	96.3	2.0	<u>93.2</u>	0.2

Table 3. Validation of mask level approaches on Fishyscapes val and RoadAnomaly. Missing results are marked with -.

Method	FS L&F		FS Static		RoadAnomaly	
	AP	FPR ₉₅	AP	FPR ₉₅	AP	FPR ₉₅
RbA	61.0	10.6	-	-	78.5	11.8
Maskomaly	-	-	68.8	15.0	80.8	12.0
EAM	52.0	20.5	87.3	2.1	66.7	13.4
UNO (ours)	74.5	6.9	96.9	0.1	82.4	9.2
RbA	70.8	6.3	-	-	85.4	6.9
Mask2Anomaly	69.4	9.4	90.5	2.0	79.7	13.5
EAM	81.5	4.2	96.0	0.3	69.4	7.7
UNO (ours)	81.8	1.3	98.0	0.04	88.5	<u>7.4</u>

6.4. Ablations

Validating components of UNO score. Table 5 validates the contribution of the two components on the UNO ensemble. In the case of synthetic negatives (top section), uncertainty outperforms negative objectness by a wide margin. This does not come as a surprise since the negative objectness is inferred from synthetic training negatives. Still, UNO greatly benefits from the ensemble of the two scores. In particular, we observe the AP improvement of 12 percentage points (pp) on RoadAnomaly. In the case of real negatives (bottom section), both components attain competitive results without a clear winner. Still, the UNO score again outperforms both components by a notable margin. For instance, UNO attains improvement of 8pp over the objectness component in terms of AP on RoadAnomaly.

Table 4. OOD detection performance on the OpenOOD CIFAR-10 and ImageNet-200. All methods train with negative data.

Method	CIFAR-10					ImageNet-200				
	Near-OOD		Far-OOD		ID Acc.	Near-OOD		Far-OOD		ID Acc.
	AUROC	FPR	AUROC	FPR		AUROC	FPR	AUROC	FPR	
MixOE	88.73	51.45	91.93	33.84	94.55	82.62	57.97	88.27	40.93	85.71
MCD	91.03	30.17	91.00	32.03	94.95	83.62	54.71	88.94	29.93	86.12
OE	94.82	19.84	96.00	13.13	94.63	84.84	52.30	89.02	34.17	85.82
UNO (ours)	95.00	18.75	97.95	9.30	94.83	85.09	51.71	89.64	36.84	86.43

Altogether, these results suggest UNO drastically improves over each of the two components.

Table 5. Validation of UNO components.

Score	Aux. Data	FS L&F		FS Static		RoadAnomaly	
		AP	FPR ₉₅	AP	FPR ₉₅	AP	FPR ₉₅
S _{Unc}	✗	71.9	8.0	95.7	0.5	70.4	9.4
S _{NO}	✗	26.6	91.1	73.9	61.1	54.2	72.3
S _{UNO}	✗	74.5	6.9	96.9	0.1	82.4	9.2
S _{Unc}	✓	74.1	4.5	72.1	1.5	66.2	8.0
S _{NO}	✓	69.0	1.6	92.6	0.14	80.4	19.8
S _{UNO}	✓	81.8	1.3	98.0	0.04	88.5	7.4

To further investigate the benefits of UNO, we analyse the correlation between the two components of the UNO ensemble. Table 6 reports the Pearson correlation coefficient of per-pixel scores on Fishyscapes and RoadAnomaly. We observe that the two UNO components are either mildly correlated or completely uncorrelated. These findings provide more insight into the performance gains of UNO can be explained by the ensemble learning (Kuncheva & Whitaker, 2003). To the best of our knowledge, this is the first work which builds uncorrelated OOD detection components atop the same recognition model.

Table 6. Pearson correlation coefficient of per-pixel scores on anomaly segmentation benchmarks.

Data	FS L&F	FS Static	RoadAnomaly
Outliers	0.27	0.01	0.13
Inliers	0.01	0.15	0.01
All	0.16	0.56	0.41

Next, we visualize the outlier detection performance in Figure 3. We show the input image, continuous OOD scores and the thresholded OOD scores. We select the threshold that yields TPR of 95%. Visual examples show that the S_{Unc} and S_{NO} have different failure modes. For example, S_{Unc} produces false positives at the borders of inlier classes while S_{NO} detects some inlier objects as outliers. Still, these failure modes cancel out with UNO score.

Impact of synthetic negatives. Table 7 shows the perfor-

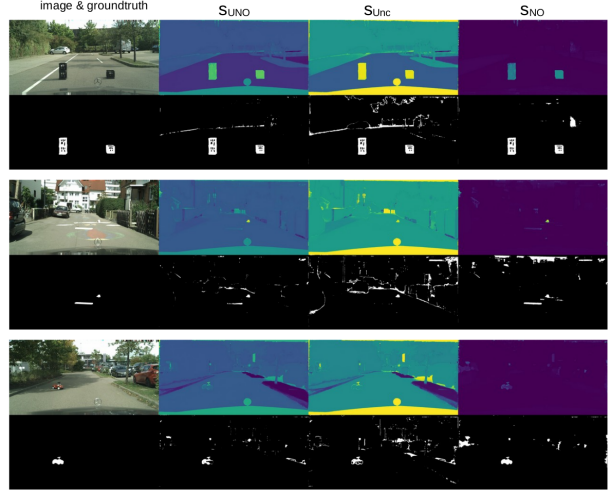


Figure 3. Three qualitative experiments on Fishyscapes L&F val (a-c). Top row shows the input image and the three anomaly scores. Bottom row shows binarized anomaly detection maps that we obtain by thresholding at 95% TPR. Please zoom-in for details.

mance of UNO depending on the source of negative training data. We experiment with random crops from inlier scenes, synthetic negatives generated by a jointly trained normalizing flow, and random instances from the ADE datasets. Training on synthetic negatives is more beneficial than training on inlier crops. For instance, training on inlier crops yields a high FPR on Fishyscapes LostAndFound. Contrary, synthetic negatives yield low FPR on all three validations sets. Still, there is a gap in anomaly detection performance between models that have and have not seen real negative data.

Table 7. Performance of UNO for different training negatives.

Training negatives	FS L&F		FS Static		RoadAnomaly	
	AP	FPR ₉₅	AP	FPR ₉₅	AP	FPR ₉₅
inliers	67.2	62.5	79.2	0.9	86.5	7.6
synthetic	74.5	6.9	96.9	0.1	82.4	9.2
ADE	81.8	1.3	98.0	0.04	88.5	7.4

Choice of real negative data We conceive a proof-of-

Table 8. Proof-of-concept experiment with pasted anomalies. We train a $M2F_{K+2}$ model on Cityscapes inliers and negatives from category A. We validate the trained model on mixed-content images with pasted anomalies from categories A and B. We observe that i) s_{NO} outperforms s_{Unc} , ii) s_{UNO} ensemble outperforms both s_{NO} and s_{Unc} alone, and iii) s_{Unc} seems to contribute the most on unseen anomalies from category B. We choose $A=sea$ and $B=chairs$.

Model	s_{Unc}		s_{NO}		s_{UNO}	
	AP_A	AP_B	AP_A	AP_B	AP_A	AP_B
$M2F_{K+2}$	59.5	51.3	95.4	76.2	96.7	82.3
$M2F_{K+1}$	16.2	11.9	-	-	-	-

concept experiment as follows. We consider ADE20K (Zhou et al., 2019) as the broad negative dataset and select two visually different categories $A = sea$ and $B = chair$. We selected the category A to be as simple as possible, and the category B to be somewhat more complicated. We fine-tune a closed-set Mask2Former trained on Cityscapes in the $K+2$ setup on mixed content images, where the negatives are sampled from the category A. We perform two validation experiments on 100 images from Cityscapes val, by pasting anomalous instances either from the category A or the category B. Table 8 reports the corresponding anomaly detection performances AP_A and AP_B . We validate all three scores s_{Unc} , s_{NO} and s_{UNO} , and compare them with the closed-set Mask2Former with $K+1$ classes. As expected, training with negative data improves anomaly detection. The method s_{Unc} generalizes well on unseen anomalies B. However, s_{NO} outperforms s_{Unc} by a large margin on anomalies from both categories. These experiments again suggest that UNO is a strong contender, since it outperforms both of its components on their own. We also note that s_{Unc} appears to contribute the most on unseen anomalies. This agrees with our intuition since s_{Unc} captures masks with uncertain mask-wide predictions.

Table 9 ablates the components of UNO over all test sets from the image-wide CIFAR-10 OpenOOD benchmark. The negative objectness score outperforms the inlier uncertainty score on the OOD datasets that are similar to the training negatives, such as TinyImageNet and Places365. Contrary, the inlier uncertainty score outperforms negative objectness on datasets that are dissimilar to the training negatives, such as CIFAR-100. Figure 2 confirms this intuition by visualizing the pre-logit embedding space using a two-dimensional tSNE plot.

7. Limitations

UNO relies on negative training data to deliver strong OOD detection performance. While standard applications offer plenty of real negative data, this might not be the case in domain-specific applications such as remote sensing and

Table 9. Ablation of the anomaly score components on the OpenOOD CIFAR-10 benchmark.

Dataset	s_{Unc}		s_{NO}	
	AUC	FPR ₉₅	AUC	FPR ₉₅
TinyIN	99.87	0.09	99.96	0.07
Places365	95.10	19.78	95.52	17.42
SVHN	99.96	0.07	99.97	0.07
MNIST	99.41	2.16	99.29	2.44
Textures	97.01	15.73	97.2	15.66
CIFAR-100	90.02	36.41	88.65	44.27

medical imaging. Still, we show that UNO can deliver strong performance when trained on synthetic negatives.

A key design choice behind UNO is the ensembling of uncorrelated OOD detection scores. This may seem like a trivial approach; however, the majority of well-established OOD detection scores are highly correlated and thus cannot benefit from ensembling. Moreover, UNO presents a clear motivation for the ensembling of inlier uncertainty and outlier objectness based on the semantic similarity between training negatives and test outliers.

8. Conclusion

Robust visual recognition is a critical component of intelligent agents in the physical world. A common strategy for outlier detection is to fine-tune the closed-set prediction model in order to increase uncertainty in negative data. We assume a more ambitious stance by introducing an additional logit for active recognition of negative data. This allows us to cast outlier detection by ensembling in-distribution uncertainty with the posterior of the negative class, which we term negative objectness. Our method works great as an extension of pixel-level approaches that decouple class-agnostic segmentation from mask-level recognition. There we first apply our ensemble to recover mask-wide anomaly scores, and then propagate them to pixels according to mask assignments. Experiments reveal state-of-the-art performance on recent image-wide and pixel-level outlier detection benchmarks with and without real negative data. Prominent future developments include improving the quality of synthetic negative data and extending our ensemble with generative predictions.

Broader impact

This paper presents work whose goal is to advance the field of Machine Learning. There are many potential societal consequences of our work, non which we feel must be specifically highlighted here.

Acknowledgements

This work has been co-funded by European Union - NextGenerationEU and Croatian Science Foundation grant IP-2020-02-5851 ADEPT.

References

- Ackermann, J., Sakaridis, C., and Yu, F. Maskomaly: Zero-shot mask anomaly segmentation. *arXiv preprint arXiv:2305.16972*, 2023.
- Bevandić, P., Krešo, I., Oršić, M., and Šegvić, S. Dense open-set recognition based on training with noisy negative images. *Image and Vision Computing*, 2022.
- Biase, G. D., Blum, H., Siegwart, R., and Cadena, C. Pixel-wise anomaly detection in complex driving scenes. In *IEEE Conference on Computer Vision and Pattern Recognition, CVPR 2021, virtual, June 19-25, 2021*, pp. 16918–16927. Computer Vision Foundation / IEEE, 2021. doi: 10.1109/CVPR46437.2021.01664.
- Bitterwolf, J., Müller, M., and Hein, M. In or out? fixing imagenet out-of-distribution detection evaluation. *arXiv preprint arXiv:2306.00826*, 2023.
- Blum, H., Sarlin, P.-E., Nieto, J., Siegwart, R., and Cadena, C. The fishyscapes benchmark: Measuring blind spots in semantic segmentation. *International Journal of Computer Vision*, 2021.
- Chan, R., Lis, K., Uhlemeyer, S., Blum, H., Honari, S., Siegwart, R., Fua, P., Salzmann, M., and Rottmann, M. Segmentmeifyoucan: A benchmark for anomaly segmentation. *arXiv preprint arXiv:2104.14812*, 2021a.
- Chan, R., Rottmann, M., and Gottschalk, H. Entropy maximization and meta classification for out-of-distribution detection in semantic segmentation. In *Proceedings of the IEEE/CVF international conference on computer vision*, pp. 5128–5137, 2021b.
- Cheng, B., Misra, I., Schwing, A. G., Kirillov, A., and Girdhar, R. Masked-attention mask transformer for universal image segmentation. In *Proceedings of the IEEE/CVF conference on computer vision and pattern recognition*, pp. 1290–1299, 2022.
- Cordts, M., Omran, M., Ramos, S., Rehfeld, T., Enzweiler, M., Benenson, R., Franke, U., Roth, S., and Schiele, B. The cityscapes dataset for semantic urban scene understanding. In *Proceedings of the IEEE conference on computer vision and pattern recognition*, pp. 3213–3223, 2016.
- Deng, J., Dong, W., Socher, R., Li, L., Li, K., and Fei-Fei, L. Imagenet: A large-scale hierarchical image database. In *IEEE Computer Society Conference on Computer Vision and Pattern Recognition CVPR*, 2009.
- Dhamija, A. R., Günther, M., and Boulton, T. E. Reducing network agnostophobia. In *Proceedings of the 32nd International Conference on Neural Information Processing Systems, NIPS’18*, pp. 9175–9186, 2018.
- Di Biase, G., Blum, H., Siegwart, R., and Cadena, C. Pixel-wise anomaly detection in complex driving scenes. In *Proceedings of the IEEE/CVF conference on computer vision and pattern recognition*, pp. 16918–16927, 2021.
- Dinh, L., Sohl-Dickstein, J., and Bengio, S. Density estimation using real NVP. In *International Conference on Learning Representations*, 2017.
- Djurisic, A., Bozanic, N., Ashok, A., and Liu, R. Extremely simple activation shaping for out-of-distribution detection. *arXiv preprint arXiv:2209.09858*, 2022.
- Galesso, S., Argus, M., and Brox, T. Far away in the deep space: Nearest-neighbor-based dense out-of-distribution detection. *CoRR*, abs/2211.06660, 2022. doi: 10.48550/ARXIV.2211.06660. URL <https://doi.org/10.48550/arXiv.2211.06660>.
- Geng, C., Huang, S.-j., and Chen, S. Recent advances in open set recognition: A survey. *IEEE transactions on pattern analysis and machine intelligence*, 43(10):3614–3631, 2020.
- Grcić, M. and Šegvić, S. Hybrid open-set segmentation with synthetic negative data. *arXiv preprint arXiv:2301.08555*, 2023.
- Grcić, M., Bevandić, P., and Šegvić, S. Dense anomaly detection by robust learning on synthetic negative data. *arXiv preprint arXiv:2112.12833*, 2021a.
- Grcić, M., Bevandić, P., and Šegvić, S. Dense open-set recognition with synthetic outliers generated by real nvp. In *16th International Joint Conference on Computer Vision, Imaging and Computer Graphics Theory and Applications, VISIGRAPP*, 2021b.
- Grcić, M., Grubišić, I., and Šegvić, S. Densely connected normalizing flows. *Advances in Neural Information Processing Systems*, 2021c.
- Grcic, M., Bevandic, P., and Segvic, S. Densehybrid: Hybrid anomaly detection for dense open-set recognition. In *European Conference on Computer Vision, ECCV 2022*. Springer, 2022.
- Grcić, M., Šarić, J., and Šegvić, S. On advantages of mask-level recognition for outlier-aware segmentation. In *Proceedings of the IEEE/CVF Conference on Computer Vision and Pattern Recognition*, pp. 2936–2946, 2023.

- Guo, C., Pleiss, G., Sun, Y., and Weinberger, K. Q. On calibration of modern neural networks. In *International conference on machine learning*, pp. 1321–1330. PMLR, 2017.
- Hawkins, D. *Identification of outliers*. Monographs on applied probability and statistics. Chapman and Hall, London, 1980. ISBN 041221900X.
- He, K., Zhang, X., Ren, S., and Sun, J. Deep residual learning for image recognition. In *Proceedings of the IEEE conference on computer vision and pattern recognition*, pp. 770–778, 2016.
- Hendrycks, D. and Gimpel, K. A baseline for detecting misclassified and out-of-distribution examples in neural networks. *arXiv preprint arXiv:1610.02136*, 2016.
- Hendrycks, D. and Gimpel, K. A baseline for detecting misclassified and out-of-distribution examples in neural networks. In *5th International Conference on Learning Representations, ICLR 2017, Toulon, France, April 24-26, 2017, Conference Track Proceedings*. OpenReview.net, 2017.
- Hendrycks, D., Mazeika, M., and Dietterich, T. Deep anomaly detection with outlier exposure. *arXiv preprint arXiv:1812.04606*, 2018.
- Hendrycks, D., Basart, S., Mazeika, M., Zou, A., Kwon, J., Mostajabi, M., Steinhardt, J., and Song, D. Scaling out-of-distribution detection for real-world settings. *arXiv preprint arXiv:1911.11132*, 2019a.
- Hendrycks, D., Mazeika, M., Kadavath, S., and Song, D. Using self-supervised learning can improve model robustness and uncertainty. *Advances in neural information processing systems*, 32, 2019b.
- Jung, S., Lee, J., Gwak, D., Choi, S., and Choo, J. Standardized max logits: A simple yet effective approach for identifying unexpected road obstacles in urban-scene segmentation. In *Proceedings of the IEEE/CVF International Conference on Computer Vision*, pp. 15425–15434, 2021.
- Kendall, A. and Gal, Y. What uncertainties do we need in bayesian deep learning for computer vision? *Advances in neural information processing systems*, 30, 2017.
- Kirichenko, P., Izmailov, P., and Wilson, A. G. Why normalizing flows fail to detect out-of-distribution data. In Larochelle, H., Ranzato, M., Hadsell, R., Balcan, M., and Lin, H. (eds.), *Advances in Neural Information Processing Systems*, 2020.
- Krizhevsky, A., Hinton, G., et al. Learning multiple layers of features from tiny images. 2009.
- Kuncheva, L. I. and Whitaker, C. J. Measures of diversity in classifier ensembles and their relationship with the ensemble accuracy. *Machine Learning*, 2003.
- Lakshminarayanan, B., Pritzel, A., and Blundell, C. Simple and scalable predictive uncertainty estimation using deep ensembles. *Advances in neural information processing systems*, 30, 2017.
- Lee, K., Lee, H., Lee, K., and Shin, J. Training confidence-calibrated classifiers for detecting out-of-distribution samples. In *International Conference on Learning Representations*, 2018.
- Li, F., Zhang, H., xu, H., Liu, S., Zhang, L., Ni, L. M., and Shum, H.-Y. Mask dino: Towards a unified transformer-based framework for object detection and segmentation. In *CVPR*, 2023.
- Liang, C., Wang, W., Miao, J., and Yang, Y. Gmmseg: Gaussian mixture based generative semantic segmentation models. In Koyejo, S., Mohamed, S., Agarwal, A., Belgrave, D., Cho, K., and Oh, A. (eds.), *Advances in Neural Information Processing Systems 35: Annual Conference on Neural Information Processing Systems 2022, NeurIPS 2022, New Orleans, LA, USA, November 28 - December 9, 2022*, 2022.
- Liang, S., Li, Y., and Srikant, R. Enhancing the reliability of out-of-distribution image detection in neural networks. *arXiv preprint arXiv:1706.02690*, 2017.
- Lin, T.-Y., Maire, M., Belongie, S., Hays, J., Perona, P., Ramanan, D., Dollár, P., and Zitnick, C. L. Microsoft coco: Common objects in context. In *Computer Vision—ECCV 2014: 13th European Conference, Zurich, Switzerland, September 6-12, 2014, Proceedings, Part V 13*, pp. 740–755. Springer, 2014.
- Lis, K., Nakka, K., Fua, P., and Salzmann, M. Detecting the unexpected via image resynthesis. In *Proceedings of the IEEE/CVF International Conference on Computer Vision*, pp. 2152–2161, 2019.
- Liu, W., Wang, X., Owens, J., and Li, Y. Energy-based out-of-distribution detection. *Advances in neural information processing systems*, 33:21464–21475, 2020.
- Liu, Z., Lin, Y., Cao, Y., Hu, H., Wei, Y., Zhang, Z., Lin, S., and Guo, B. Swin transformer: Hierarchical vision transformer using shifted windows. In *Proceedings of the IEEE/CVF international conference on computer vision*, pp. 10012–10022, 2021.
- Malinin, A. and Gales, M. Predictive uncertainty estimation via prior networks. *Advances in neural information processing systems*, 31, 2018.

- Mukhoti, J. and Gal, Y. Evaluating bayesian deep learning methods for semantic segmentation. *arXiv preprint arXiv:1811.12709*, 2018.
- Nalisnick, E., Matsukawa, A., Teh, Y. W., Gorur, D., and Lakshminarayanan, B. Do deep generative models know what they don’t know? In *International Conference on Learning Representations*, 2019.
- Nayal, N., Yavuz, M., Henriques, J. F., and Güney, F. Rba: Segmenting unknown regions rejected by all. In *Proceedings of the IEEE/CVF International Conference on Computer Vision*, pp. 711–722, 2023.
- Neal, L., Olson, M., Fern, X., Wong, W.-K., and Li, F. Open set learning with counterfactual images. In *Proceedings of the European Conference on Computer Vision (ECCV)*, 2018.
- Neuhof, G., Ollmann, T., Rota Buló, S., and Kotschieder, P. The mapillary vistas dataset for semantic understanding of street scenes. In *Proceedings of the IEEE international conference on computer vision*, pp. 4990–4999, 2017.
- Rai, S. N., Cermelli, F., Fontanel, D., Masone, C., and Caputo, B. Unmasking anomalies in road-scene segmentation. In *Proceedings of the IEEE/CVF International Conference on Computer Vision*, pp. 4037–4046, 2023.
- Ruff, L., Kauffmann, J. R., Vandermeulen, R. A., Montavon, G., Samek, W., Kloft, M., Dietterich, T. G., and Müller, K. A unifying review of deep and shallow anomaly detection. *Proc. IEEE*, 109(5):756–795, 2021.
- Sakaridis, C., Dai, D., and Gool, L. V. ACDC: the adverse conditions dataset with correspondences for semantic driving scene understanding. In *2021 IEEE/CVF International Conference on Computer Vision, ICCV 2021, Montreal, QC, Canada, October 10-17, 2021*, pp. 10745–10755. IEEE, 2021.
- Shalev, G., Adi, Y., and Keshet, J. Out-of-distribution detection using multiple semantic label representations. In Bengio, S., Wallach, H. M., Larochelle, H., Grauman, K., Cesa-Bianchi, N., and Garnett, R. (eds.), *Advances in Neural Information Processing Systems 31: Annual Conference on Neural Information Processing Systems 2018, NeurIPS 2018, December 3-8, 2018, Montréal, Canada*, pp. 7386–7396, 2018.
- Tao, L., Du, X., Zhu, X., and Li, Y. Non-parametric outlier synthesis. *arXiv preprint arXiv:2303.02966*, 2023.
- Tian, Y., Liu, Y., Pang, G., Liu, F., Chen, Y., and Carneiro, G. Pixel-wise energy-biased abstention learning for anomaly segmentation on complex urban driving scenes. In *European Conference on Computer Vision*, pp. 246–263. Springer, 2022.
- Vaze, S., Han, K., Vedaldi, A., and Zisserman, A. Open-set recognition: A good closed-set classifier is all you need? *arXiv preprint arXiv:2110.06207*, 2021.
- Vojir, T., Šipka, T., Aljundi, R., Chumerin, N., Reino, D. O., and Matas, J. Road anomaly detection by partial image reconstruction with segmentation coupling. In *Proceedings of the IEEE/CVF International Conference on Computer Vision*, pp. 15651–15660, 2021.
- Vojir, T., Sochman, J., Aljundi, R., and Matas, J. Calibrated out-of-distribution detection with a generic representation. *arXiv preprint arXiv:2303.13148*, 2023.
- Wei, H., Xie, R., Cheng, H., Feng, L., An, B., and Li, Y. Mitigating neural network overconfidence with logit normalization. In *International Conference on Machine Learning*, pp. 23631–23644. PMLR, 2022.
- Yang, J., Wang, H., Feng, L., Yan, X., Zheng, H., Zhang, W., and Liu, Z. Semantically coherent out-of-distribution detection. In *Proceedings of the IEEE/CVF International Conference on Computer Vision*, pp. 8301–8309, 2021.
- Yu, Q. and Aizawa, K. Unsupervised out-of-distribution detection by maximum classifier discrepancy. In *Proceedings of the IEEE/CVF international conference on computer vision*, pp. 9518–9526, 2019.
- Yu, Q., Wang, H., Qiao, S., Collins, M., Zhu, Y., Adam, H., Yuille, A., and Chen, L.-C. k-means Mask Transformer. In *ECCV*, 2022.
- Zendel, O., Honauer, K., Murschitz, M., Steininger, D., and Domínguez, G. F. Wilddash - creating hazard-aware benchmarks. In Ferrari, V., Hebert, M., Sminchisescu, C., and Weiss, Y. (eds.), *Computer Vision - ECCV 2018 - 15th European Conference, Munich, Germany, September 8-14, 2018, Proceedings, Part VI*, volume 11210 of *Lecture Notes in Computer Science*, pp. 407–421. Springer, 2018. URL https://doi.org/10.1007/978-3-030-01231-1_25.
- Zhang, H., Li, A., Guo, J., and Guo, Y. Hybrid models for open set recognition. In Vedaldi, A., Bischof, H., Brox, T., and Frahm, J. (eds.), *Computer Vision - ECCV 2020 - 16th European Conference, Glasgow, UK, August 23-28, 2020, Proceedings, Part III*, volume 12348 of *Lecture Notes in Computer Science*, pp. 102–117. Springer, 2020.
- Zhang, J., Fu, Q., Chen, X., Du, L., Li, Z., Wang, G., Han, S., Zhang, D., et al. Out-of-distribution detection based on in-distribution data patterns memorization with modern hopfield energy. In *The Eleventh International Conference on Learning Representations*, 2022.

- Zhang, J., Inkawhich, N., Linderman, R., Chen, Y., and Li, H. Mixture outlier exposure: Towards out-of-distribution detection in fine-grained environments. In *Proceedings of the IEEE/CVF Winter Conference on Applications of Computer Vision*, pp. 5531–5540, 2023a.
- Zhang, J., Yang, J., Wang, P., Wang, H., Lin, Y., Zhang, H., Sun, Y., Du, X., Zhou, K., Zhang, W., et al. Openood v1.5: Enhanced benchmark for out-of-distribution detection. *arXiv preprint arXiv:2306.09301*, 2023b.
- Zhao, Z., Cao, L., and Lin, K. Revealing distributional vulnerability of explicit discriminators by implicit generators. *CoRR*, 2021.
- Zhou, B., Zhao, H., Puig, X., Xiao, T., Fidler, S., Barriuso, A., and Torralba, A. Semantic understanding of scenes through the ade20k dataset. *International Journal of Computer Vision*, 127:302–321, 2019.

A. Appendix.

A.1. Baselines and related work

We compare UNO with the following baselines and related work. In the image-wide setup we consider training methods that utilize negative data: OE (Hendrycks et al., 2018), MCD (Yu & Aizawa, 2019), UDG (Yang et al., 2021) and MixOE (Zhang et al., 2023a).

We compare UNO with related anomaly segmentation methods in two disciplines: with and without use of real negative data. We consider the following pixel-level methods: Maximum Entropy (Chan et al., 2021b), Image Resynthesis (Lis et al., 2019), JSRNet (Vojir et al., 2021), MC Dropout (Kendall & Gal, 2017), ODIN (Liang et al., 2017), Max softmax (Hendrycks & Gimpel, 2017), SML (Jung et al., 2021), Embedding Density (Blum et al., 2021), NFlowJS (Grcić et al., 2021b), SynDHybrid (Grcić & Šegvić, 2023), cDNP (Galesso et al., 2022), SynBoost (Di Biase et al., 2021), Prior Entropy (Malinin & Gales, 2018), OOD Head (Bevandić et al., 2022), Void Classifier (Blum et al., 2021), Dirichlet prior (Malinin & Gales, 2018), DenseHybrid (Grcić et al., 2022) and PEBAL (Tian et al., 2022).

Additionally, we compare UNO with recent methods that build on top of Mask2Former architecture: Mask2Anomaly (Rai et al., 2023), Maskomaly (Ackermann et al., 2023), EAM (Grcić et al., 2023) and RbA (Nayal et al., 2023).

A.2. Alternative implementation of the outlier posterior

Table 10. Comparison of the K+2-way classifier with the OOD head on top of Mask2Former architecture on Fishyscapes val and RoadAnomaly.

Method	Anomaly score	FS L&F			FS Static			RoadAnomaly		
		AP	AUROC	FPR ₉₅	AP	AUROC	FPR ₉₅	AP	AUROC	FPR ₉₅
K+2-way classifier	S _{UNO}	81.8	98.7	1.3	98.0	100.0	0.0	88.5	97.8	7.4
K-way classifier & OOD head	S _{UNO}	81.4	98.4	5.3	89.0	99.8	0.3	80.6	97.3	10.6
K-way classifier & OOD head	S _{Unc}	77.8	98.2	2.2	86.4	99.2	1.6	76.1	95.9	8.4
K-way classifier & OOD head	S _{NO}	79.9	98.1	7.3	88.3	99.7	0.3	74.5	94.9	25.2

Table 11. Comparison of the K+1-way classifier with the binary OOD head on top of ResNet-18 on OpenOOD Cifar-10. We use UNO as the anomaly score.

Method	Near-OOD		Far-OOD	
	AUC	FPR ₉₅	AUC	FPR ₉₅
K+1-way classifier	95.00	18.75	97.95	9.30
K-way classifier & OOD head	94.23	19.31	97.76	11.12

We analyse a different approach to model the negative objectness. We model the outlier posterior $P(y_{NO}|\mathbf{z})$ with an additional out-of-distribution head as proposed in (Bevandić et al., 2022). In addition to the cross-entropy loss over K classes we introduce another cross-entropy loss term to train the out-of-distribution head to discriminate between inliers and outliers. This way the closed set classifier ends up with K classes and is not affected by the negative data. When applied to the mask-wide recognition architecture, the OOD head has 3 outputs 1) inlier, 2) outlier and 3) no-object. Table 10 shows comparison of the K+2-way classifier proposed in the main paper with a K+1-way classifier and a 3-way OOD head and ablation of UNO components in the pixel-wise anomaly detection setup. Table 11 shows comparison of the K+1-way classifier with a K-way classifier and a binary OOD head on OpenOOD Cifar-10. This approach produces suboptimal results with respect to the K+1 classifier, e.g. K+2 classifier in the case of mask-wide recognition architecture). However, it shows that our anomaly score can work in architectural setups.